THE ASTROPHYSICAL JOURNAL, 341: 722–732, 1989 June 15

THE ABUNDANCE GRADIENT ACROSS THE GALAXY NGC 2997

J. R. WALSH
Kapteyn Astronomical Institute
AND
JEAN-RENÉ ROY
Département de Physique, and Observatoire Astronomique du mont Mégantic, Université Laval
Received 1988 August 31; accepted 1988 December 2

ABSTRACT

The fiber optics coupling aperture-plate system (FOCAP) of the Anglo-Australian Observatory was used to obtain low-dispersion spectra of 49 H II regions across the galaxy NGC 2997. Problems with employing fiber optics for spectrophotometry are discussed. Correlations between line ratios used as diagnostics for physical conditions and abundances in H II regions are identical to those found by McCall, Rybski, and Shields for a large number of giant H II regions in 26 galaxies. The O/H radial abundance gradient in NGC 2997 was derived using the calibration of the index ([O II] + [O III])/Hβ. The gradient and the mean metallicity of NGC 2997 are comparable to those of M51. There is significant dispersion in ([O II] + [O III])/Hβ and [O III]/Hβ at any given galactocentric distance. No N^+/O^+ gradient is observed, and the mean value of this ratio is identical to that of Galactic H II regions.

Subject headings: galaxies: abundances — galaxies: individual (NGC 2997) — nebulae: abundances — nebulae: H II regions

I. INTRODUCTION

The abundances of elements vary from galaxy to galaxy and within galaxies (Pagel and Edmunds 1981; Pagel 1985). In disk galaxies the mean $\langle O/H \rangle$ averaged over individual galaxies increases with the masses and luminosities of galaxies but decreases as their gas fractions increase. Abundances are correlated with the stellar surface density (McCall 1982); they can be used to trace the mass distribution in galaxies, the initial mass function, and the stellar formation rate.

In gas-rich galaxies, abundances are derived from H II regions or supernova remnant (SNR) spectra (Pagel 1985), while in ellipticals absorption features in the continuum spectra such as the Mg_2 index are related to the abundance of Fe. Radial abundance gradients appear common enough to throw some light on the dissipation mechanisms acting at galaxy formation. Abundances are high at the center and decrease outward. Although the data are scanty, the amplitudes of these gradients appear to depend on the morphological type of the galaxies. The gradients are steep ($\Delta \log \langle O/H \rangle / \Delta \rho \approx 1$) in normal spirals; they are weaker in barred spirals (Alloin *et al.* 1981) and possibly very small in irregulars or Magellanic systems. The gradients inferred for [Fe/H] in elliptical galaxies are small ($\sim$0.3 in the log), but their slopes appear similar, at least in the rather bright ellipticals sampled so far; see, for example, Baum, Thomsen, and Morgan (1986) and Couture and Hardy (1988).

Our knowledge of abundances in galaxies is very limited. For ellipticals it is not easy to deconvolve the effects of different stellar populations from varying metallicities; furthermore high signal-to-noise ratio (S/N) spectra are very difficult to obtain away from the center. For disk galaxies, what we know is based on very few H II regions per galaxy; for example, the abundance gradient of M 101, one of the best studied objects, was established from the spectra of 18 objects (Evans 1986). To determine the gradient in our own Milky Way, Shaver *et al.* (1983) based their study on 67 H II regions. Consequently very little is known about the azimuthal dependence of abundances, the scatter at a given radius, or of the relations between abundances and dynamical features such as bars or rings.

In order to increase significantly the number of H II regions sampled in any given galaxy, we have applied the technique of multiobject spectroscopy. We have used the fiber optics coupling aperture-plate system (FOCAP) of the Anglo-Australian Observatory (Gray 1983) to obtain the spectra of a large number of H II regions in a disk galaxy. Our observations confirm that fiber optics-fed spectrographs can be used for spectrophotometric work. We were able to determine the abundance gradient in the spiral galaxy NGC 2997 based on spectra of 49 H II regions obtained in less than 4 hr of 4 m telescope observing time. Due to difficulties described in the following sections, we consider our spectra not as accurate as those obtained using conventional slit spectroscopy; but our attempt was successful enough to present the results, and to propose improved procedures for doing spectrophotometry using fiber optics.

II. OBSERVATIONS

Low-dispersion spectra of the H II regions of NGC 2997 were obtained using the RGO spectrograph (25 cm camera) and the image photon counting system (IPCS) on the 3.9 m Anglo-Australian Telescope during the night of 1987 December 26–27. The FOCAP system with its bundle of 64 fibers of 300 μm core diameter (2″ on sky) was employed to feed the spectrograph. A 250 lines per mm grating was used in the first-order blaze to collimator for a dispersion of 156 Å mm^{-1}. Due to limitations in the computer external memory, we reduced the resolution to 10 Å in order to maintain a broad spectral coverage from 3400 Å to 7300 Å. At this resolution one needs to do multiple line-profile fitting to separate the [N II] 6548 and 6584 Å lines from Hα. This procedure leads to larger errors in the [N II] flux estimates when S/N ratio is low. Total integration time for our observations was 14,000 s.

NGC 2997 is a beautiful southern spiral galaxy belonging to a loose group of galaxies (Peterson 1978) located at about 10 Mpc. More references to works related to this object can be found in Roy and Walsh (1987). The H II regions for fiber spectroscopy were chosen from Milliard and Marcelin (1981) who have published an atlas of its H II regions. The positions of many H II regions were measured, using a PDS, from a prime focus *R* band plate obtained by David Malin at the f/3.3 prime focus of the Anglo-Australian Telescope. The 49 H II regions observed are shown in Figure 1. One more fiber was centered on the nucleus, and seven fibers were located on empty sky; however, one sky fiber turned out to be probably contaminated by a faint star or galaxy, and the sky spectrum was constructed from the mean of the six others.

Spectrophotometry using fiber optics presents some problems which must be addressed.

(*1*) *Small aperture.*—To derive abundances from the spectra of H II regions, it is important to use line fluxes integrated over the whole of H II regions (Evans 1986; Roy and Walsh 1988). It is known that line ratios show significant spatial fluctuations (Roy and Walsh 1986, 1987; Roy, Belley, and Walsh 1989). Most of the H II regions that we observed in NGC 2997 have diameters in the range of 5″–10″, much bigger than our 2″ apertures. To increase the area sampled by each fiber, the telescope was set in a continuous scan motion, by moving it on a circle of 1″ radius at a rate of one full circle per 50 s. Convolved with seeing of 1″.5–2″, the effective sampling area was $\sim 6''$ in diameter. (With larger fibers we would get better efficiency since more of the H II regions would be sampled and there would be no need to scan the telescope. However, the spectral resolution would be degraded beyond the resolution needed to resolve the [N II] lines at 6548 Å and 6584 Å from Hα.)

(*2*) *Spectral response calibration.*—The small and fixed size of fibers (e.g., 2″ on sky in the present case) also makes the observation of standard spectrophotometric stars difficult; spectra are hard to rely on when obtained away from the zenith. Added to the difficulty of knowing within 1″ the position on the fiber of the calibration star, atmospheric differential refraction put more constraints on the usual flux calibration procedure. The need to ensure proper flux calibration made us choose NGC 2997 as a target galaxy because we could rely on previous spectrophotometry of a chain of H II regions along the main northern arm of the galaxy (Roy and Walsh 1987). Our fiber sample had four regions in common with our imaging spectroscopy, i.e., region 11 corresponds to NGC 2997B, 13 to 2997E, 20 to 2997I, and 23 to part of region 2997L (cf. Fig. 1 of Roy and Walsh 1987). Spectra corresponding to the same size as the area scanned by each fiber were extracted from the ASPECT data cube, and compared with the fiber spectra. Final relative flux calibration of the fiber data was achieved by using a mean calibration derived from this comparison.

(*3*) *Cross-talk.*—Some of the light coming out from one fiber at the slit entrance of the spectrograph is slightly scattered to the adjacent fibers in the spectrograph. We measured this effect to be about 1%–1.5%. To reduce the contamination induced by such cross-talk, we chose a set of H II regions not too different in surface brightness and avoided positioning fibers from very bright objects adjacent to faint ones at the slit.

(*4*) *Sky subtraction.*—Fibers have a relative total transmission which varies from one to another. A sky exposure was used to calibrate the response and to check that it does not change by replugging or moving the fiber when special care is taken. All fibers were renormalized to a reference fiber. Sky subtraction was done by using a mean sky averaged over six sky fibers.

(*5*) *Color effect.*—For bundles of fibres constructed from the same supply of fibers, the spectral responses of fibers of equal length are identical. Nevertheless we found a slight color effect when comparing the sky spectra of different fibers. This effect arises from the extraction procedure of the individual spectra from the long-slit spectrum of all H II regions. The extraction is done by matching an aperture around each H II region spectrum. Because it is impossible to correct perfectly for the *S*-distortion of the IPCS, one has to fit the upper and lower boundaries of each spectrum with a low-order polynomial. Therefore it is extremely difficult to ensure that the shape of this window matches perfectly any given spectrum; actually it may cut into pixels having some flux from the adjacent fibers at some wavelengths. This does not affect too seriously line fluxes; however it makes the continuum spectra unreliable. Because of their fixed geometry, CCDs would not be affected by this problem.

(*6*) *Total budget error.*—The reader may wonder how we can ever achieve reliable spectrophotometry. It should be realized that each of these problems account for uncertainties of the order of 2% to 3%. Comparison between the spectra of our regions 11, 27, 25, and 24 in common with H II regions No. 2, No. 1, No. 5, and No. 3 of Edmunds and Pagel (1984) shows slight differences which can be explained by the different sampling area of both studies; otherwise the agreement is good. We estimate the uncertainty in the line ratios that we derive to be about 15% to 20%. Diagnostic diagrams shown in Figure 3 will support this. Overall the quality of the spectra we obtained in NGC 2997 is inferior to that obtained with conventional slit spectroscopy, but important scientific results can be derived.

We feel that the quality of spectrophotometry done through fiber optics can be improved drastically by employing a detector with a better defined geometry than the IPCS to avoid introducing color effects in the extraction procedure. Also flux calibration could be made more reliable when observing standard spectrophotometric stars by scanning an elongated area along the parallactic angle to ensure that light of all wavelengths gets into the fiber, or better by installing a wide-field atmospheric dispersion corrector on the telescope. The value of using the multifiber technique for the spectrophotometry of H II regions resides in the scientific interest in doing 50 H II regions at once and in the scientific benefits resulting. A similar application of the fiber technique has been done recently by Zaritsky, Elston, and Hill (1989); they used the MX multiobject spectrometer to obtain high-resolution spectra of 55 H II regions in M33 in order to derive velocity and excitation measurements.

Data reduction was done using standard procedures. An interactive procedure for fitting continuum and emission lines was used to derive the line fluxes $F(\lambda)$ expressed in units of $F(\mathrm{H}\beta) = 100$. The line spectra were corrected for interstellar reddening by comparing the $\mathrm{H}\alpha/\mathrm{H}\beta$ ratios to the theoretical Balmer decrement as given by Brocklehurst (1971) for a density of 100 cm^{-3} but after adding 2 Å of equivalent width to the Hβ emission line to compensate for the underlying Balmer absorption (cf. McCall, Rybski, and Shields, hereafter MRS and Roy and Walsh 1987). The reddening correction was done by also considering the temperature of the H II regions as calibrated by Stasińska *et al.* (1981) for the ([O II] + [O III])/Hβ; however the effect of temperature is small for this sample of

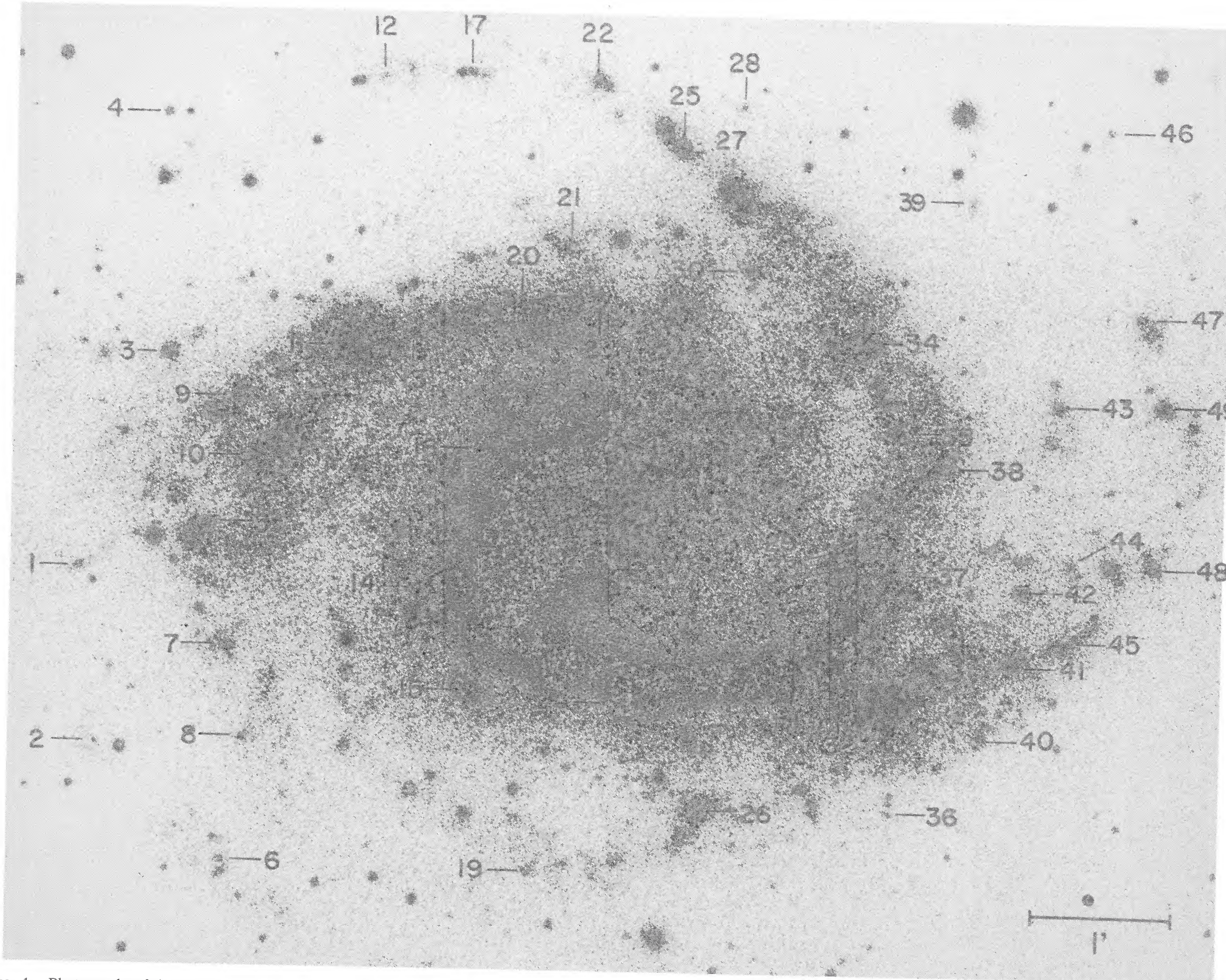

FIG. 1.—Photographs of the southern spiral galaxy NGC 2997 (Sc) obtained by David Malin at the f/3.3 prime focus of the 3.9 m Anglo-Australian Telescope. The positions of the 49 H II regions observed with the FOCAP system are indicated. The small black dot just above the 1′ scale bar gives the approximate size of the area scanned by each fiber.

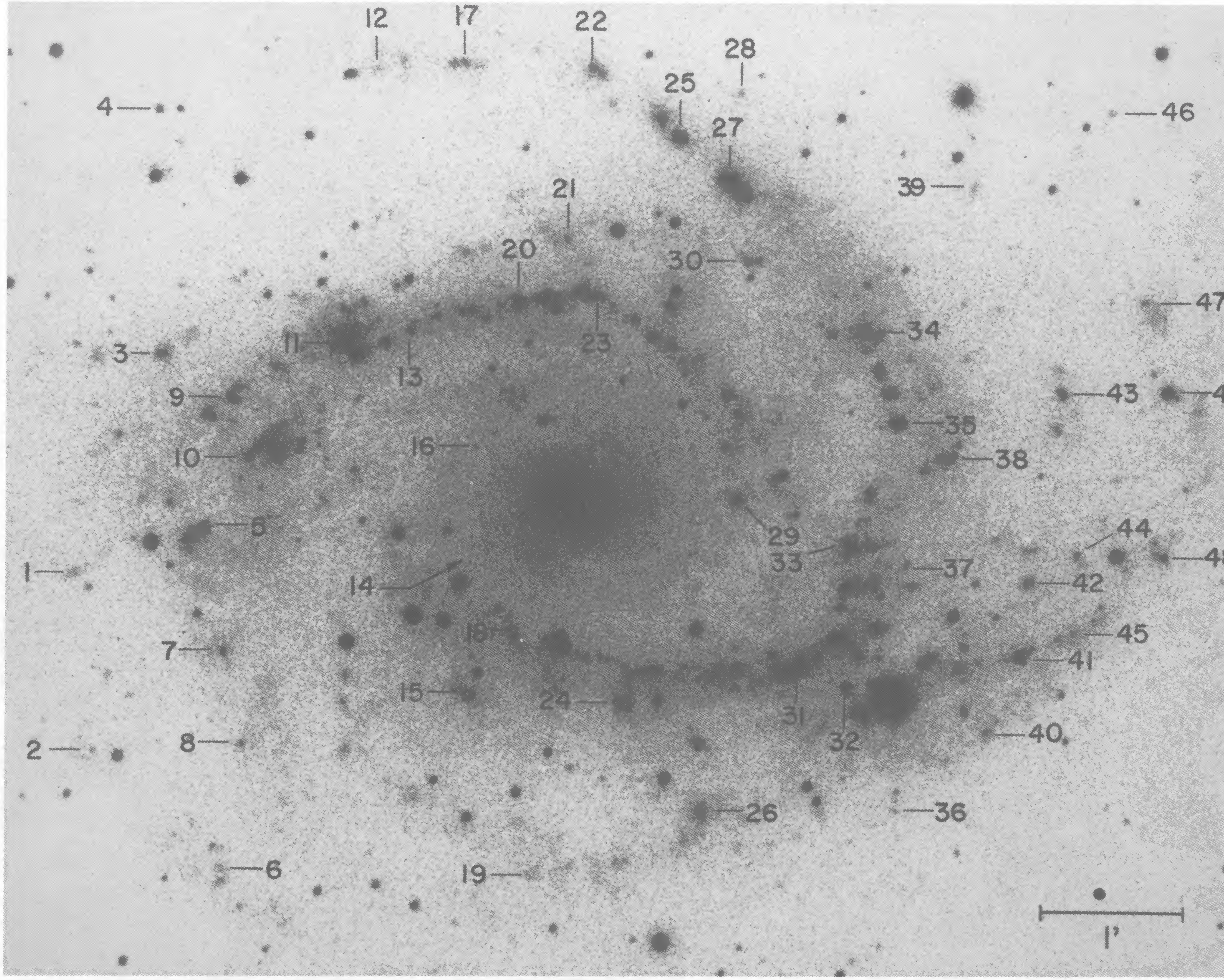

FIG. 1.—Photographs of the southern spiral galaxy NGC 2997 (Sc) obtained by David Malin at the f/3.3 prime focus of the 3.9 m Anglo-Australian Telescope. The positions of the 49 H II regions observed with the FOCAP system are indicated. The small black dot just above the 1′ scale bar gives the approximate size of the area scanned by each fiber.

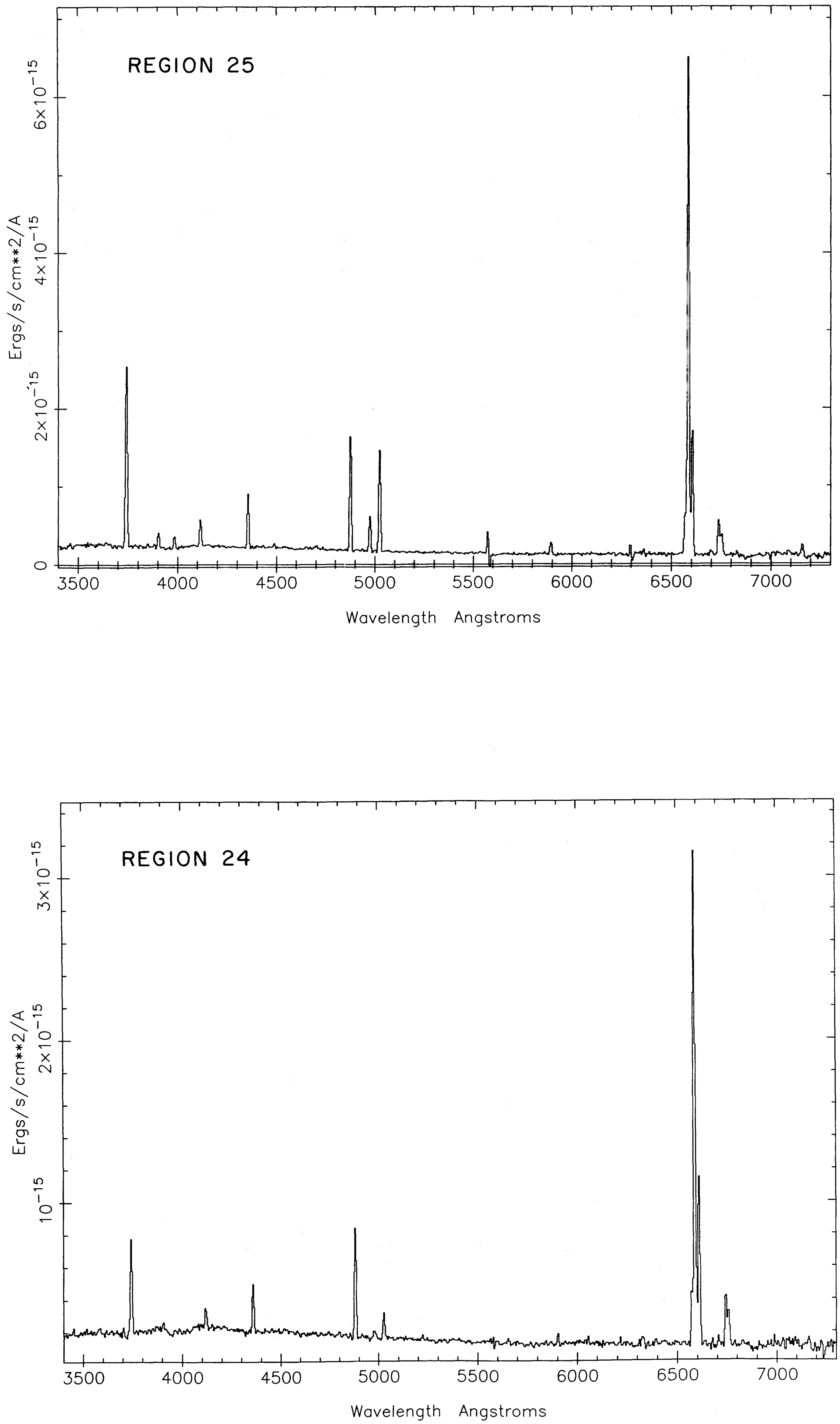

FIG. 2.—Examples of spectra obtained with FOCAP. No correction for interstellar extinction has been applied.

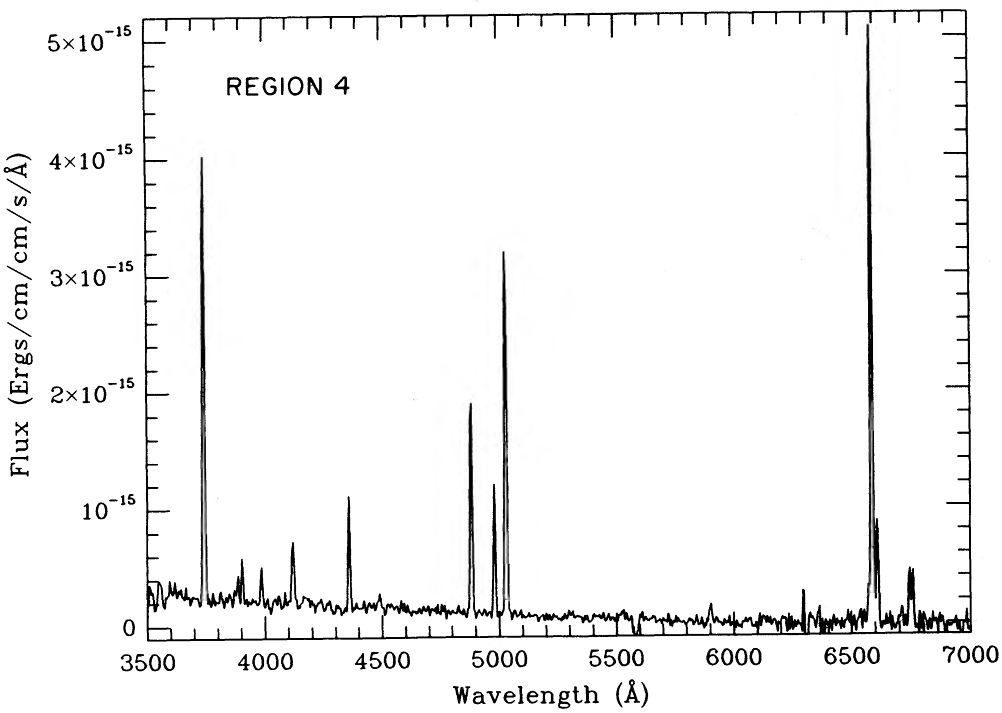

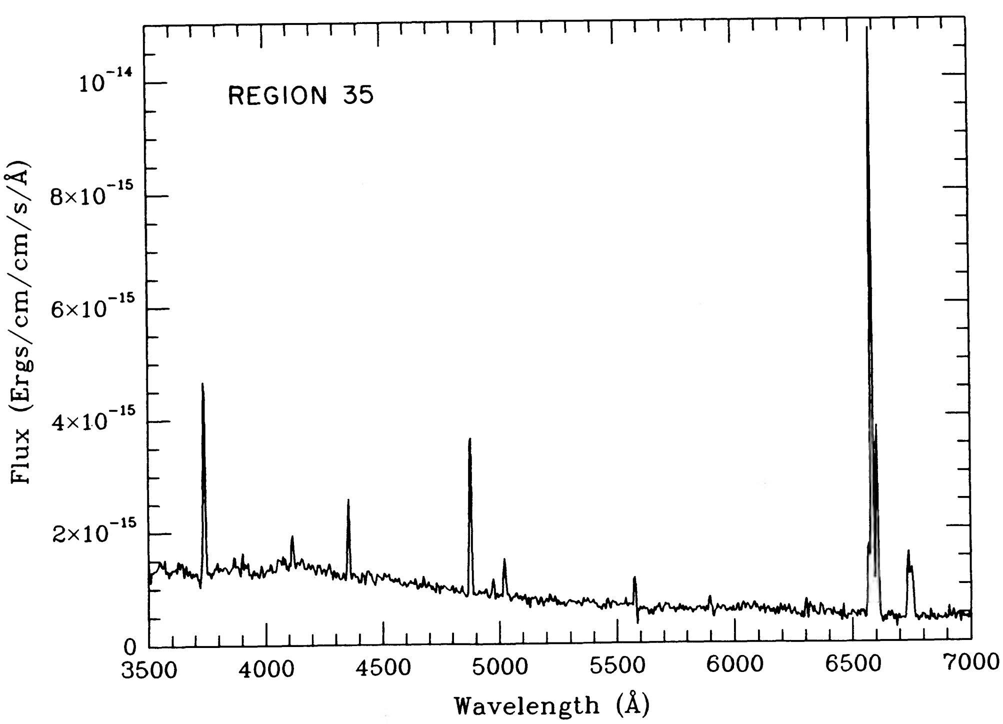

FIG. 2—*Continued*

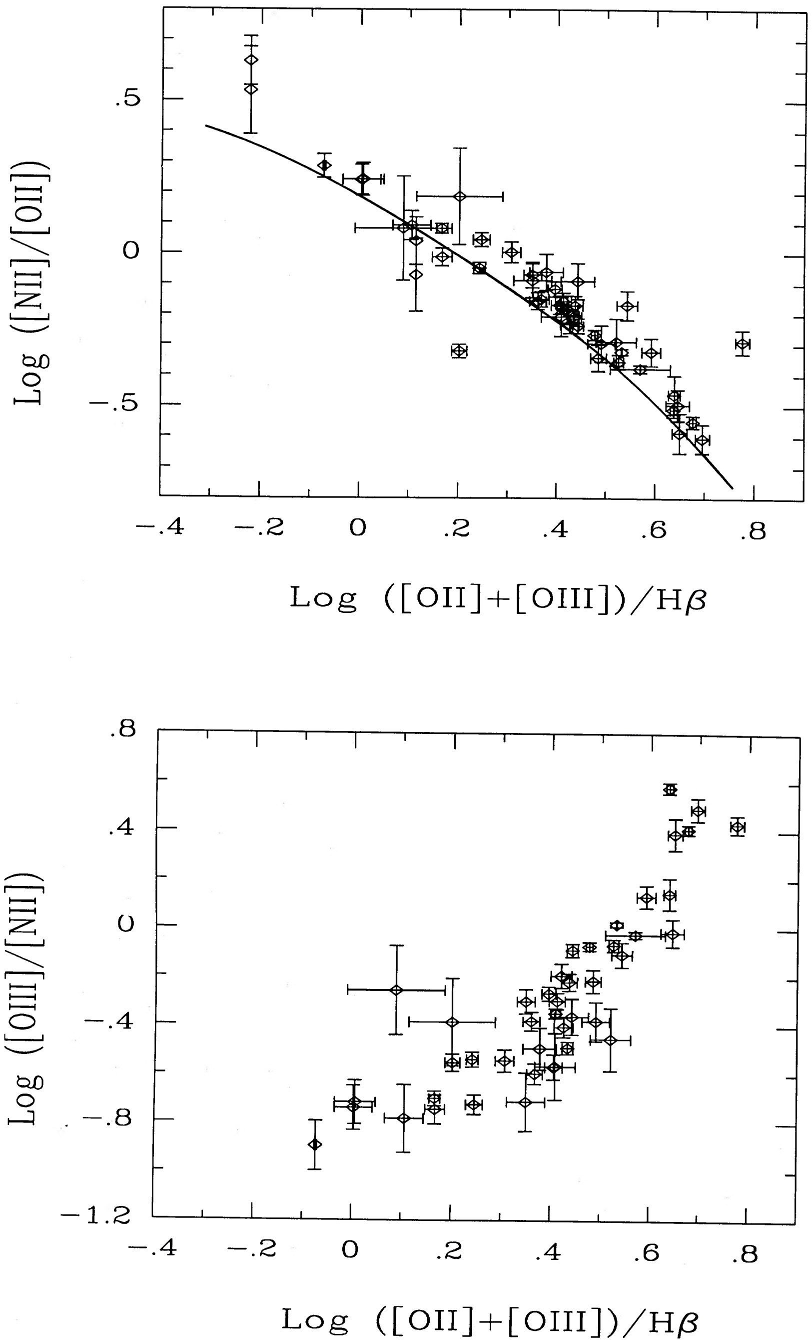

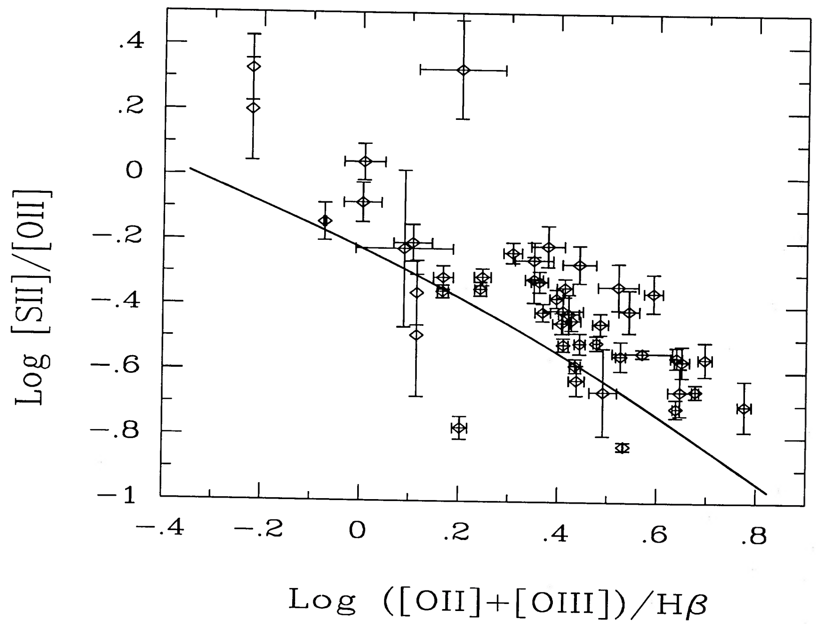

FIG. 3.—Diagnostic diagrams of log [N II]/[O II], log [S II]/[O II] and log [O III]/[N II] vs. the sequencing index log ([O II] + [O III])/Hβ. The curves correspond to the predicting equations found by McCall, Rybski, and Shields (1985) for 99 giant H II regions in 26 galaxies.

b) *Diagnostic Diagrams*

We have calculated several line ratios after correction for reddening. A table of these line ratios is available from the authors. We have plotted our data for several line ratios using ([O II] + [O III])/Hβ as a sequencing parameter. MRS have shown that this line ratio is the best parameter for sequencing the spectra of H II regions, and that the oxygen abundance is the most important determinant of the emission spectrum of an H II region. Figure 3 shows [N II]/[O II], [S II]/[O II], and [O III]/[N II] versus this parameter. The tight relationships shown by these sequences imply that the majority of the nebulae are ionization-bounded. Two points appear off the main sequence in the [N II]/[O II] plot; because of the problems of disentangling the [N II] lines from Hα, we do not consider that these points are significantly off. Similar comments apply to the [S II]/[O II] plot because of weak [S II] lines.

The trends that we find in NGC 2997 are identical to those found by MRS (shown by the thick curves in Fig. 3*a* and 3*b*), except that some of our points tend to fall above the sequence found by MRS, but well within its dispersion. Part of this difference could be due to using different spectrophotometric calibrations stars and reddening law to MRS. Furthermore our sample of H II regions differs from that of MRS. While their sample is biased toward very large and bright H II regions, we have included in our sample many objects which are not very conspicuous, at least in the continuum (Fig. 1). Finally the MRS sequence is based on spectra of H II regions from 26 different galaxies, while ours refers to only one galaxy. Nevertheless the tight sequence shown by [N II]/[O II] demonstrates (i) that spectrophotometry with fibers gives reliable line fluxes, (ii) that the trend observed among the brightest H II regions from several galaxies is maintained within the various H II regions of an individual galaxy. We have looked at several other correlations. No obvious trend comes out apart from the correlations already found by MRS, except a correlation between log F(Hβ) and log W(Hβ) which has a coefficient of correlation of 0.52.

c) *Radial Gradients in NGC 2997*

We calculated the galactocentric distances and azimuthal positions of the H II regions by assuming a 40° inclination of the galaxy disk to the plane of sky, and a position angle of the line of nodes of 110° (Milliard and Marcelin 1981). We used a value for the de Vaucouleurs isophotal radius ρ_0 of 4'.35 (McCall 1982). Line ratios which show systematic radial variations are the excitation indicator [O III]/Hβ (Fig. 4*a*), [O III]/[N II], and the oxygen abundance indicator ([O II] + [O III])/Hβ (Fig. 4*b*). Other ratios such as [N II]/[S II] and [N II]/Hα display slight diminishing trends with radial distances. There is no systematic variation of c, the logarithmic extinction at Hβ, as a function of radius. All ratios display large and significant scatter at any given galactocentric distance.

Since no direct measurement of the electron temperatures is available, we have to rely on the semiempirical method of Pagel *et al.* (1979) to derive abundances. This method has been widely used (e.g., MRS; Evans 1986; Garnett and Shields 1987; Vilchez *et al.* 1988); it is based on the result that larger values of [(O II] + [O III])/Hβ are correlated with higher electron temperatures and lower abundances of oxygen. This calibration has been refined by Edmunds and Pagel (1984), MRS, and Dopita and Evans (1986). Figure 5 shows the [O/H] abundance gradients derived from the calibrations of Edmunds and Pagel (1984: EP84) and Dopita and Evans (1986: DE86); employing the MRS calibration would lead to values similar to those of Edmunds and Pagel for the range of [O/H] found in NGC 2997.

Using the T_e values for each H II region derived from the calibration of ([O II] + [O III])/Hβ versus T_e by Stasińska *et al.*, we derived the N^+/O^+ ionic abundances; this is usually recognized as being close to N/O, although infrared observations give systematic differences between those two ratios; see, for example, Rubin (1986). Errors can seriously affect this ratio; an error of 500 K in the temperature at 5000 K produces a 36% error in the N^+/O^+ ratio; equivalent figures are 22% at 6000 K, 17% at 7000 K, and 13% at 8000 K. Figure 6 shows that there is little systematic gradient in N^+/O^+ in NGC 2997. A similar result was found in M81 by Garnett and Shields (1987). The mean N^+/O^+ ratio in NGC 2997 (0.09 ± 0.02) is slightly smaller than that of M81. The values of N^+/O^+ are very similar to those found by Shaver *et al.* (1983) for Galactic H II regions.

IV. DISCUSSION

For a given range of values of ([O II] + [O III])/Hβ, Dopita and Evans (1986) results lead to a much smaller range of oxygen abundances than Edmunds and Pagel (1984). Nonetheless, the abundance gradient is obvious. For the range of radial distances 0.2 to 1.2ρ_0, O/H falls by a factor of almost 10 following EP84 (Δ log [O/H]/$\Delta\rho \approx 0.9$), or three following DE86 (Δ log [O/H]/$\Delta\rho \approx 0.4$). The run of O/H abundance versus radius can be compared to that observed in other galaxies such as in Pagel (1985), although these are based on very few points. The O/H abundances and gradient of NGC 2997 are very similar to those of M51. The gradient in NGC 2997 is about half as steep as that of M101 (Evans 1986); the mean $\langle$O/H$\rangle$ for NGC 2997 is higher than for M101. M81 is another well-sampled galaxy (Garnett and Shields 1987); the range of abundances and $\langle$O/H$\rangle$ are slightly larger in NGC 2997 compared to M81.

A striking, but not too surprising, result of our study is the significant scatter of ([O II] + [O III])/Hβ and [O III]/Hβ found at any given galactocentric radius. Zaritsky, Elston, and Hill (1989) have also observed more scatter in the excitation values at a given radius in M33 than can be accounted by observational errors. There is an uncertainty of about 0.2 dex (for EP84) and 0.1 dex (for DE86) in [O/H] determinations (shown as vertical bars in Fig. 5) based on the ([O II] + [O III])/Hβ; thus part of this scatter could indicate abundance fluctuations. Giant H II regions are sites of vigorous star formation, massive stars with winds, Wolf-Rayet stars, and supernova activity. These phenomena last for several million years leading to local enrichment. The general dynamics of the galaxy (differential rotation and turbulence) will take several more million years to diffuse the local abundance enhancements, well after the disappearance of the H II complexes. The lifetimes of H II regions are much shorter than the mean galactic rotation time. Fluctuations in abundances observed in H II regions reflect the very recent enhancement of abundances, which in turn depends on supernova rate and the number of massive stars. However the scatter in ([O II] + [O III])/Hβ at fixed radius might reflect ionizing star temperature differences rather than abundance fluctuations; photoionization models and better spectra will be needed to

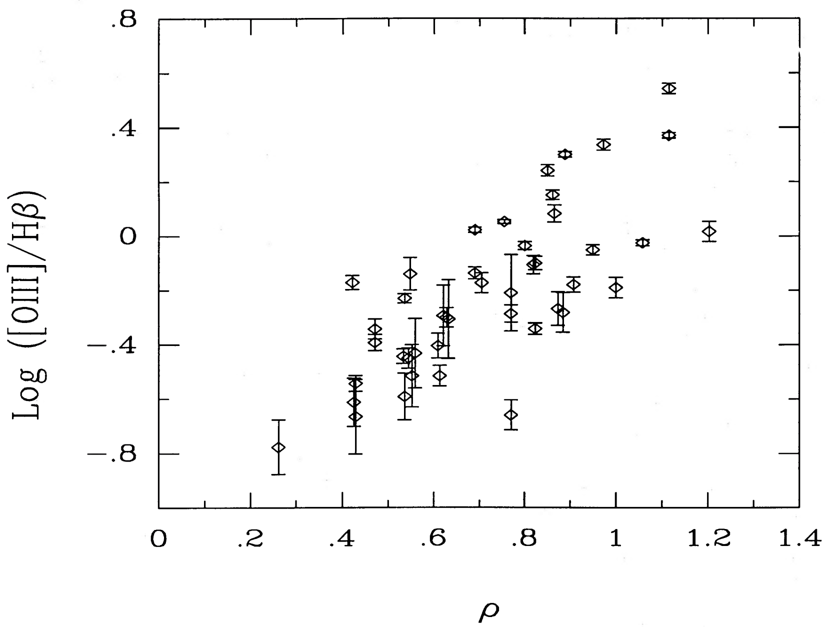

FIG. 4a

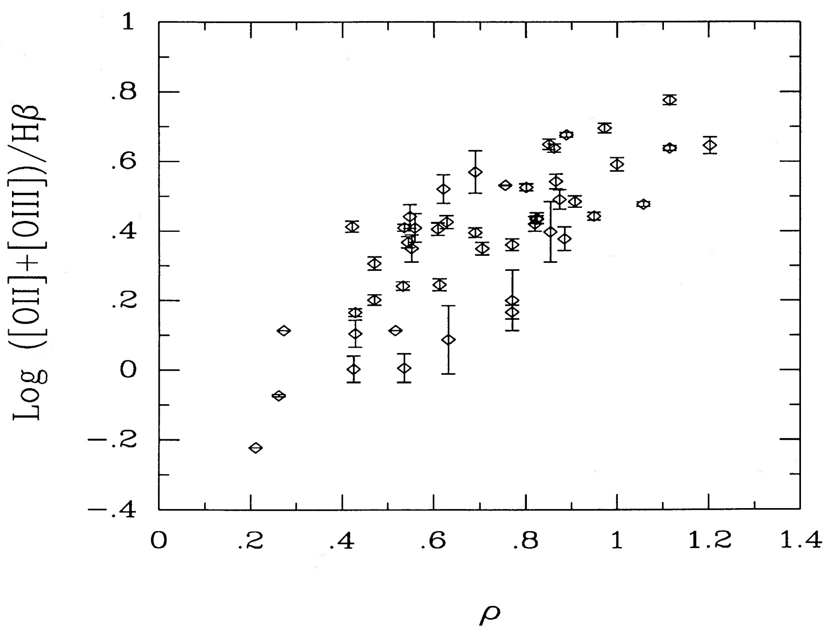

FIG. 4b

FIG. 4.—(*a*) The quantity of log [O III]/Hβ plotted against the normalized isophotal radius in NGC 2997. (*b*) The quantity of log ([O II] + [O III])/Hβ vs. the normalized isophotal radius.

confirm whether the scatter means real abundance fluctuations.

Extinction is not found to be a function of galactocentric distance or of ([O II] + [O III]/Hβ. This is in contrast with the earlier finding (Roy and Walsh 1987) of a trend between excitation and extinction. This discrepancy illustrates the differences between integrated spectra and single pixel spectra derived from spectral maps. In the latter case fluctuations in extinction within a given H II region are observed; the extinction-excitation correlation is then statistical in the sense that nebular regions with higher excitation are associated with the hottest (and youngest) stars which in turn are found preferentially close to more dusty environments. In integrated spectra such as those obtained with FOCAP, these fluctuations are wiped out. Furthermore the variations of reddening from one region to another dominate. Although we found slight correlations between reddening and excitation in all objects that we have mapped spectroscopically (NGC 1365, 1566, 2997, and 5253) when considering single pixel maps, the correlation disappears when the spectral data are summed over whole H II regions to produce integrated spectra; this result is consistent with the FOCAP data.

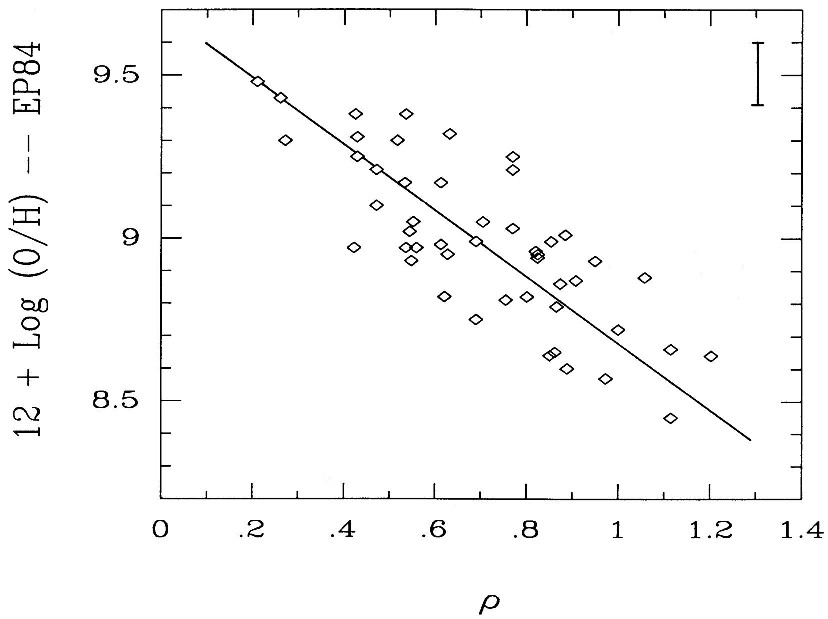

FIG. 5a

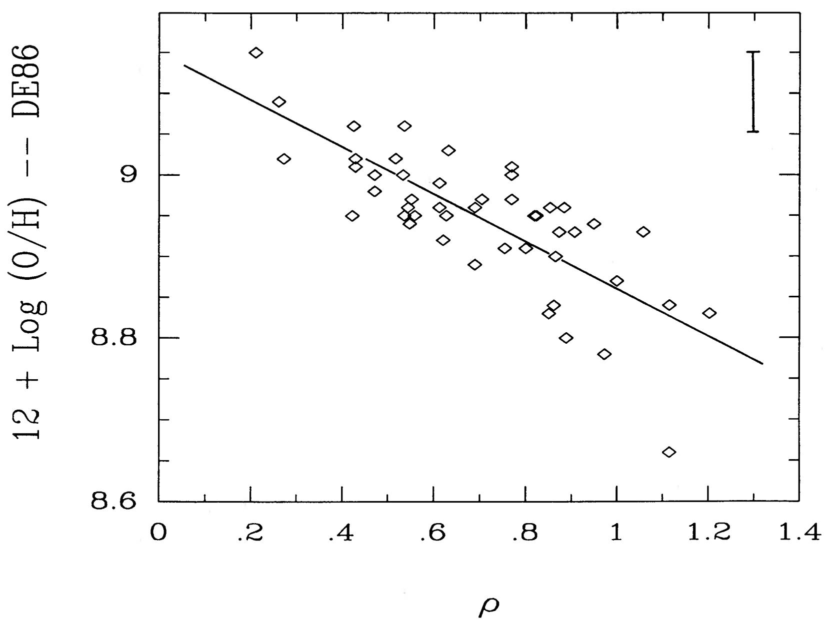

FIG. 5b

FIG. 5.—(a) The gradient in oxygen abundance across NGC 2997 using the calibration of ([O II] + [O III])/Hβ by Edmunds and Pagel (1984); the line regression corresponds to the equation $12 + \log(O/H) = 9.60 - (0.87 \pm 0.01)\rho$. (b) The same gradient using the calibration of Dopita and Evans (1986); the line corresponds to the equation $12 + \log(O/H) = 9.20 - (0.29 \pm 0.03)\rho$.

V. SUMMARY

We have identified the difficulties of doing spectrophotometry using optical fibers to feed a spectrograph. The main problem is the difficulty of correcting for the system spectral response by observing standard spectrophotometric stars because of the small aperture defined by fibers on the sky; it is suggested to scan the calibration star along the parallactic angle. The ideal long-term solution is to install a wide-field atmospheric dispersion corrector. A second limitation arose when extracting the individual H II regions spectra from the long-slit image; the difficulty of correctly matching the remnant uncorrected *S*-distortion of the IPCS introduced color effects. This effect should not arise with CCD detectors where the geometry is well defined and stable. These difficulties were overcome in most parts, and we were able to conduct a multiobject spectrophotometric study of 49 H II regions in the southern galaxy NGC 2997.

Our results are the following.

1. The correlations between line ratios [N II]/[O II] and [S II]/[O II] with ([O II] + [O III])/Hβ are identical to those found by MRS for a large number of giant H II regions observed in 26 different galaxies.

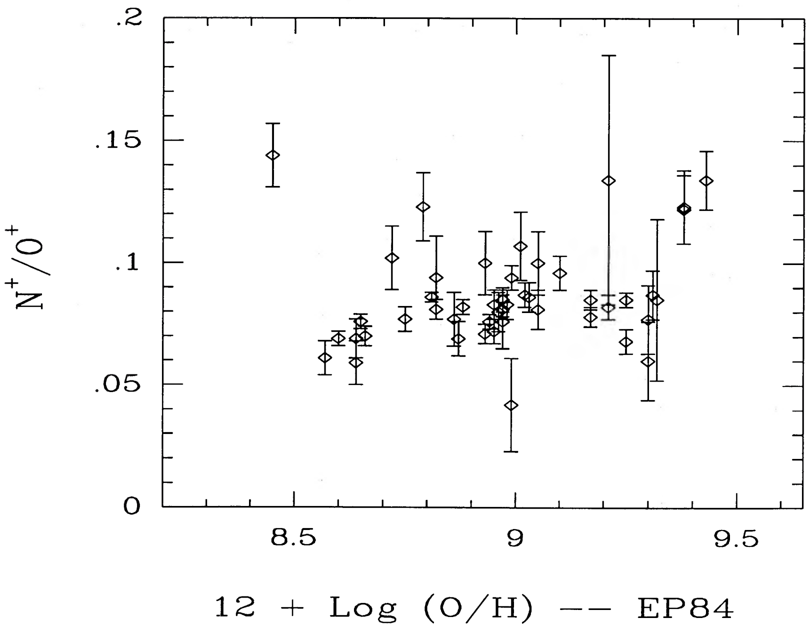

FIG. 6.—The ratio N^+/O^+ plotted against 12 + log O/H using the calibration of ([O II] + [O III])/Hβ by Edmunds and Pagel (1984).

2. We have found the spectral signature of Wolf-Rayet stars in four H II regions.

3. Using the semiempirical method of Pagel *et al.* (1979) to derive the relative abundance, gives an abundance gradient in [O/H] of about 1.0 dex over the range 0.2 to 1.2 isophotal radius; the mean metallicity is high, comparable to that of M51. The recent calibration by Dopita and Evans (1986) leads to a smaller range of O/H, thus a flatter gradient.

4. There are significant variations of the abundance indicator ([O II] + [O III])/Hβ and of the excitation [O III]/Hβ at any given galactocentric distance.

5. No gradient in N^+/O^+ is found, and the mean value of $\langle N^+/O^+ \rangle$ in NGC 2997 is similar to that found for Galactic H II regions by Shaver *et al.* (1983).

We thank the Australian Telescope Allocation Committee for assigning time on the Anglo-Australian Telescope for this project. We are indebted to John Lucy and Ray Sharples for assistance and comments on handling spectra obtained with FOCAP. Louis Noreau helped in producing the figures of this paper. The system FOCAP was designed and built by Peter Gray. Part of this work was done while one of us (J. R. W.) was on staff at the Anglo-Australian Observatory. This investigation was funded in part by the Natural Sciences and Engineering Research Council of Canada.

REFERENCES

Alloin, D., Edmunds, M. G., Linblad, P. O., and Pagel, B. E. J. 1981, *Astr. Ap.*, **101**, 377.
Baum, W. A., Thomsen, B., and Morgan, B. L. 1986, *Ap. J.*, **301**, 83.
Brocklehurst, M. 1971, *M.N.R.A.S.*, **153**, 471.
Couture, J., and Hardy, E. 1988, *A.J.*, **96**, 867.
Dopita, M. A., and Evans, I. N. 1986, *Ap. J.*, **307**, 431 (DE86).
Edmunds, M. G., and Pagel, B. E. J. 1984, *M.N.R.A.S.*, **211**, 507 (EP84).
Evans, I. N. 1986, *Ap. J.*, **309**, 544.
Garnett, D. R., and Shields, G. A. 1987, *Ap. J.*, **317**, 82.
Gray, P. M. 1983, in *Instrumentation in Astronomy V*, ed. A. Boksenberg and D. L. Crawford (*Proc. SPIE*, **445**), p. 57.
McCall, M. L. 1982, Ph.D. thesis, University of Texas, Austin.
McCall, M. L., Rybski, P. M., and Shields, G. A. 1985, *Ap. J. Suppl.*, **57**, 1 (MRS).
Milliard, B., and Marcelin, M. 1981, *Astr. Ap.*, **95**, 59.
Pagel, B. E. J. 1985, in *Production and Distribution of C, N, O Elements*, ed. I. J. Danziger, F. Matteucci, and K. Kjar (Garching: ESO), p. 155.
Pagel, B. E. J., and Edmunds, M. G. 1981, *Ann. Rev. Astr. Ap.*, **19**, 77.
Pagel, B. E. J., Edmunds, M. G., Blackwell, D. E., Chun, M. S., and Smith, G. 1979, *M.N.R.A.S.*, **189**, 95.
Peterson, C. J. 1978, *Ap. J.*, **226**, 75.
Roy, J.-R., Belley, J., and Walsh, J. R. 1989, *A.J.*, in press.
Roy, J.-R., and Walsh, J. R. 1986, *M.N.R.A.S.*, **223**, 39.
———. 1987, *M.N.R.A.S.*, **228**, 883.
———. 1988, *M.N.R.A.S.*, **234**, 977.
Rubin, R. H. 1986, *Ap. J.*, **309**, 334.
Seaton, M. J. 1979, *M.N.R.A.S.*, **187**, 73P.
Shaver, P. A., McGee, R. X., Newton, L. M., Danks, A. C., and Pottasch, S. R. 1983, *M.N.R.A.S.*, **204**, 53.
Stasińska, G., Alloin, D., Collin-Souffrin, and Joly, M. 1981, *Astr. Ap.*, **93**, 362.
Vilchez, J. M., Pagel, B. E. J., Diaz, A. I. Terlevich, E., and Edmunds, M. G. 1988, *M.N.R.A.S.*, **235**, 633.
Zaritsky, D., Elston, R., and Hill, J. M. 1989, *A.J.*, **97**, 97.

JEAN-RENÉ ROY: Département de physique, Université Laval, Québec, Qc G1K 7P4, Canada

JEREMY R. WALSH: Kapteyn Astronomical Institute, Postbus 800, 9700 AV Groningen, The Netherlands